Chapter 8

Lead and Zinc Sintering

Baojun Zhao

Additional information is available at the end of the chapter

http://dx.doi.org/10.5772/54618

1. Introduction

1.1. Background of lead and zinc production

Galena (PbS) and sphalerite (ZnS) are the major ore minerals for Pb and Zn respectively. Pyrometallurgical processing of Pb and Zn metals usually includes four stages: ore dressing, smelting, drossing and refining. Sinter – blast furnace route is one of the most important smelting technologies which was adopted from iron and steel industries. Lead-rich sinter is treated in lead blast furnace to produce lead metal. Sometimes it is difficult to separate lead and zinc minerals, Imperial Smelting Process is used to treat mixed zinc-lead ores for production of lead and zinc metals simultaneously. A typical flowsheet of lead-zinc smelter is shown in Figure 1 [1].

Imperial Smelting Furnace (ISF) is also called zinc blast furnace which was developed for mixed zinc-lead ores. Charges to the furnace are lump sinter, hot briquettes, and coke. Slag and lead are continuously tapped from the bottom of the furnace into a forehearth where separation occurs. The slag containing zinc overflows to the fuming plant to recover zinc. Liquid lead containing copper and precious metals is transferred by ladle to the decopperizing plant. Zinc vapor generated in the furnace enters the lead splash condenser where it is quenched and absorbed by fine lead droplets splashed by the rotors. The hot lead containing zinc is pumped from the condenser to a brick-lined cooling launder fitted with immersion boiler panels. On cooling the recirculating lead stream, crude zinc is released and separated by specific gravity from lead. The lead is then returned to the splash condenser.

The smelting of lead and zinc includes oxidisation (sintering) and reduction stages. The main chemical reactions involved are

Sintering: $2PbS + 3O_2 = 2PbO + 2SO_2$

$2ZnS + 3O_2 = 2ZnO + 2SO_2$

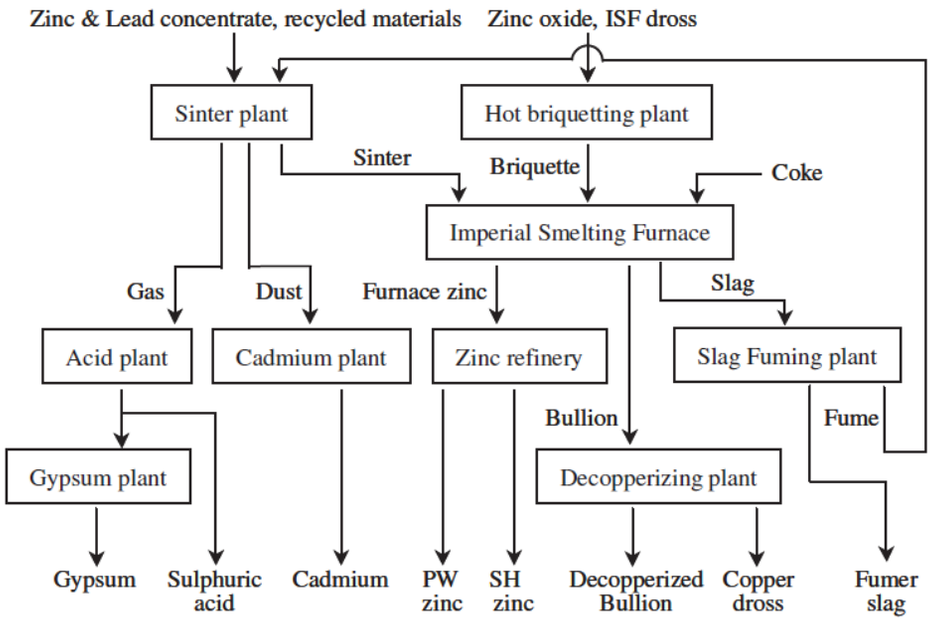

Figure 1. A typical flowsheet of lead-zinc smelter [1]

Reduction: $2PbO + C = 2Pb + CO_2$

$PbO + CO = Pb + CO_2$

$2ZnO + C = 2Zn + CO_2$

$ZnO + CO = Zn + CO_2$

1.2. Why sintering

Lead and zin metals are produced in blast furnace. In a blast furnace, ore, coke and flux are continuously supplied through the top of the furnace, while air (sometimes with oxygen enrichment) is blown into the lower section of the furnace, so that the chemical reactions take place throughout the furnace as the material moves downward. The downward flow of the ore and flux in contact with an upflow of hot, carbon monoxide-rich combustion gases is a countercurrent exchange process. Fine particles cannot be used as the feed of a blast furnace because they will be blown out by the high pressure gas flow. Zinc and lead sulphides occur as small particles in the rock. There are only a few percentage of zinc and/or lead present in commercial ores and they have to be concentrated by mineral dressing before smelting. The fine particles produced during the dressing cannot be fed into a blast furnace directly. The suitable feed for a blast furnace should be strong lump made of oxides which can be obtained by sintering. The main goals of sintering are 1) produce hard oxide lump; 2) remove sulphur; 3) produce strong SO_2 for acid plant.

1.3. Sintering process

Sinter is the primary feedstock for blast furnace to produce lead and zinc metals and it is obtained by the oxidation sintering of fine particulate zinc/lead sulphide concentrates in

updraught sinter machines. A typical flowsheet of sinter process is shown in Figure 2. The product is a partially fused porous agglomerate, which is crushed and large lump material is fed to the blast furnace. Fine sinter material is recycled or returned to the sinter feed to act as a support for fresh feed. The return sinter and fresh feed (sulphide concentrate, fluxes, fume, sludge) are agglomerated to form granulated spherical feed with 5-10 mm diameter to sintering machine.

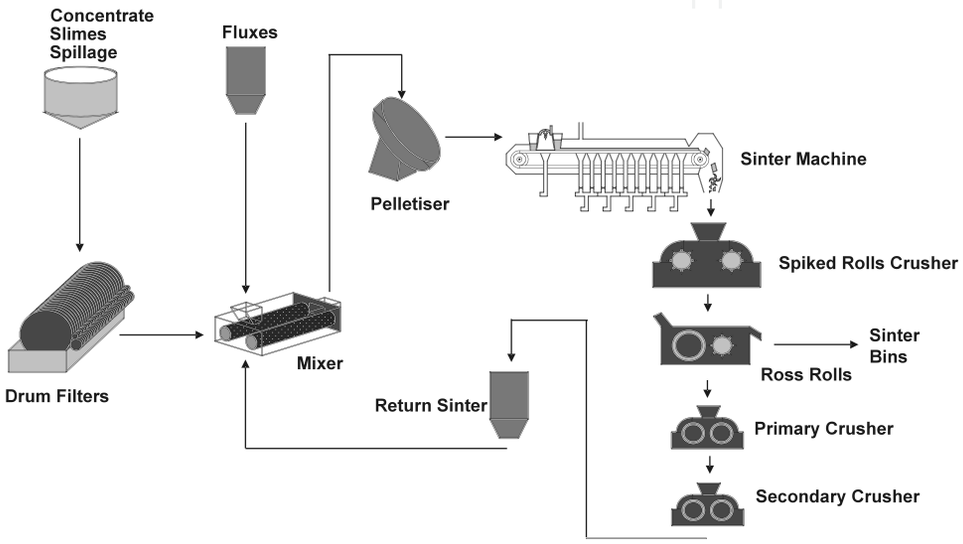

Figure 2. A typical flowsheet of sinter process

Sample	Composition (wt%)								
	Zn	Pb	Fe	CaO	SiO_2	Al_2O_3	MgO	Cu	S
concentrate	33-42	15-19	4-9	1-5	2-6	0.7-2	0.2-1	0.5-1.3	19-26
sinter	37-44	15-22	7-12	3-6	3-5	0.6-2	0.2-1	0.6-1.2	0.3-1.6

Table 1. Composition ranges of concentrate and sinter for ISF

Sample	Composition (wt%)								
	Zn	Pb	Fe	CaO	SiO_2	Al_2O_3	MgO	Cu	S
concentrate	4-7	38-46	6-8	2-11	5-13	0.7-2	0.2-0.6	0.6-0.7	9-12
sinter	4-9	36-52	8-14	6-12	7-11	0.8-2.4	0.3-2	0.3-1.2	1.1-3.4

Table 2. Composition ranges of concentrate and sinter for lead blast furnace

2. Sinter quality and conditions affecting sinter-making

2.1. Sinter quality

To obtain high productivity in all packed bed processes, it is essential to maintain a high bed voidage. In lead and zinc blast furnace this high bed voidage is achieved through careful control of sinter characteristics, ensuring in particular that the sinter does not deform under the process conditions experienced in the furnace. The quality of sinter is associated with its properties such as macrostructure and microstructure, and represented quantitatively by softening temperature.

2.1.1. Macrostructure

The macrostructures of the sinter varied from partially-fused feed granules to well-fused material. Most sinters were well-fused and physical strength of these sinters is high at room temperature. An example of a well-fused lead sinter is presented in Figure 3a. Presence of original feed granules (see Figure 3b) in some sinters indicates that during sintering these materials did not attain high temperature. Similarly, there are also well-fused part (Figure 4a) and partially-fused part (Figure 4b) in ISF sinter. The partially-fused or even non-fused parts of the sinter do not have required physical strength and they usually contain high level of sulphur. These sinter particles will be returned to the sinter machine as "core" of the feeds.

Figure 3. Typical macrostructures of lead sinter

2.1.2. Microstructure

Pieces of sinter lump with approximately 20mm diameter were selected from different parts of the as-received sinters. These samples were mounted, polished and carbon-coated for examination. Microstructural analysis was performed using a Phillip XL30 scanning electron microscopy (SEM). The typical microstructures of "as-received" lead sinter samples are presented in Figure 5.

In the lead sinter samples melilite [2(Ca,Pb)O (Zn,Fe,Mg)O $2(SiO_2,Al_2O_3)$], spinel [$(Zn,Fe^{2+},Mg)O\ (Fe^{3+},Al)_2O_3$], lead oxide (PbO), calcium silicate sulphate [$Ca_5(SiO_4)_2SO_4$] and

http://dx.doi.org/10.5772/54618

Figure 4. Typical macrostructures of ISF sinter

glass are found to be common phases. In addition, some other phases such as undissolved blast furnace slag, di-calcium silicate [2(Ca,Pb)O SiO_4], Pb-Zn silicate (larsenite, $PbZnSiO_4$), Pb-Ca silicate ($Pb_3Ca_2Si_3O_{11}$), lead sulphide (PbS), copper sulphide (CuS), Ca sulphates (CaO $CaSO_4$ and 2CaO $CaSO_4$), silica (SiO_2), Pb metal and Cu metal are also observed in lead sinters. Examples of the phases are shown in Figures 5a to 5d.

It is found that there are two extremes of melilite structures, high aspect ratio (length to thickness) and low aspect ratio melilite. At high volume fractions the high aspect ratio melilite forms a framework structure which is expected to support the sinter lump at high temperature in the blast furnace. Low aspect ratio melilite are always present as isolated crystals surrounded by matrix material which consists of the relict of the melt from which this phase is formed.

Inspection of a large number of lead sinter microstructures shows that structures of the lead sinters are not uniform; even within a 20mm diameter sinter granule the structure of the lead sinter can vary significantly. It can be seen from Figure 5a that framework melilite structure is present and the proportions of the low melting point matrix phases are very low in this area. However, significant proportions of lead metal, remaining blast furnace slag and sulphides are also observed in the same sample. Various structures such as framework melilite, blocky melilite, remaining blast furnace slag and lead metal can always be observed in each sample. This indicates that it is difficult to characterize lead sinter quality simply on the basis of microstructure.

Typical microstructures of the ISF sinter from different lumps are presented in Figure 6. Zincite [(Zn,Fe)O] and spinel [$(Zn,Fe^{2+},Mg)O\ (Fe^{3+},Al)_2O_3$] were found to be the major phases present in all ISF sinters. The matrix including glass, lead oxide, larsenite ($PbZnSiO_4$), di-calcium silicate [2(Ca,Pb)O SiO_4] is also present in all samples. In addition, melilite [2(Ca,Pb)O $(Zn,Fe,Mg)O\ 2(SiO_2,Al_2O_3)$] and lead-zinc sulfides are also common phases observed in the ISF sinter. The microstructure of the ISF sinter is generally determined by the shape and the arrangement of the zincite phase. There are usual two typical microstructures in the sinter lump: framework zincite and blocky zincite. In the region of the framework zincite the zincite has relatively high aspect ratio and forms continuous interlocking refractory structure (Figure 6a). In the region of the blocky zincite the zincite has relatively lower aspect ratio and exists

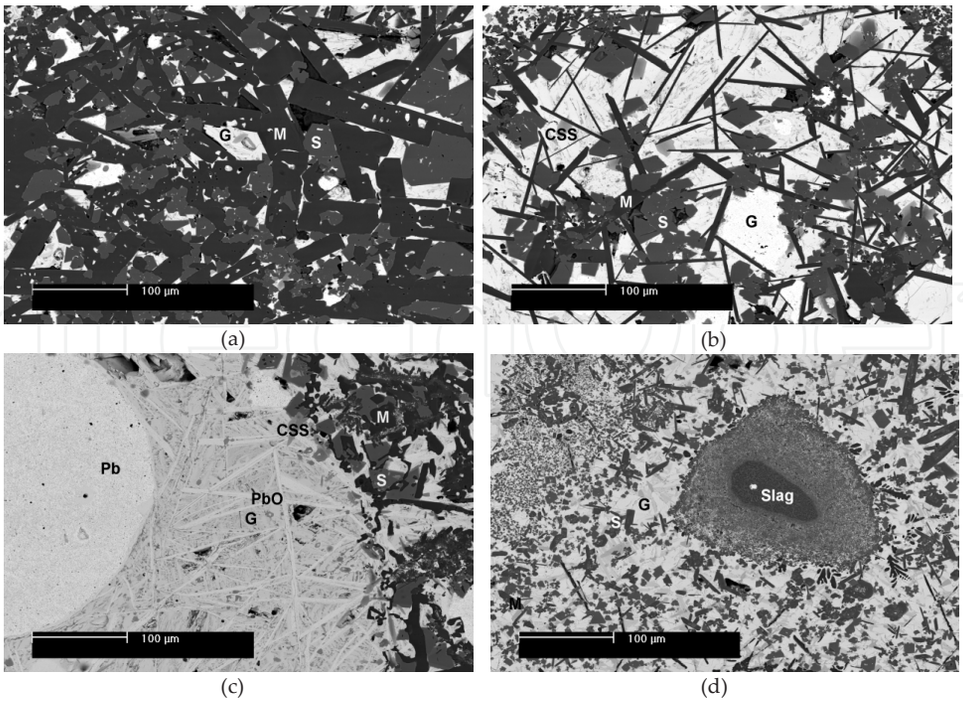

Figure 5. Typical microstructures of lead blast furnace sinter, CSS=$Ca_5(SiO_4)_2SO_4$; G=glass; M=melilite; Pb=lead metal; S=spinel [13]

as isolated phase (Figure 6b). In some of the sinters the framework zincite is dominated and in other sinters the blocky zincite is dominated.

In general, the microstructure of the ISF sinter is more uniform than that of the lead sinter. The microstructures shown in Figure 5 can be observed within a single lump of the lead sinter. However, the microstructures shown in Figure 6 are not usually to be observed within a single lump of the ISF sinter.

2.1.3. Softening temperature

The extent of the deformation is quantitatively expressed by the softening of the sinter on controlled heating rate. Softening temperature of lead sinter lump was measured in air using a vertical tube furnace shown schematically in Figure 7 [2]. The furnace was preheated to 650 ^{o}C for lead sinters and 800 ^{o}C for ISF sinters. A sinter sample with approximately 30 mm height was placed on an alumina plate and slowly raised to the hot zone of the furnace. The displacement probe (8mm OD alumina sheath with R-type thermocouple inside) was gently lowered onto the top of the sample. An aluminum plate is attached to the alumina sheath so that the total mass of the probe is approximately 235 g for lead sinters and 400 g for ISF sinters. The displacement meter was positioned on the top of the aluminum plate, which is fixed to the probe. The displacement meter was set to about half of its shaft's travel to allow for expansion and softening of the sample. The displacement meter gauge was set to zero. The furnace temperature was increased with a uniform heating rate of 400 degrees per hour, which was controlled by a programmable temperature controller (Philips KS 40). Initially the sinter

http://dx.doi.org/10.5772/54618

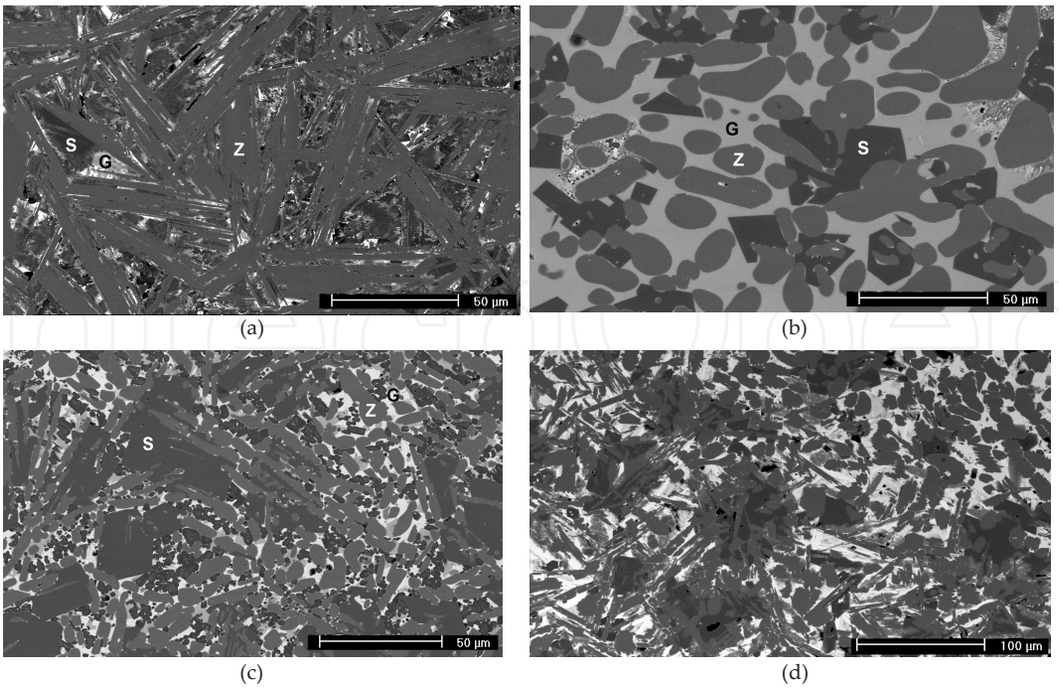

Figure 6. Typical microstructures of ISF sinter, G=glass; S=spinel; Z=ZnO [3]

was observed to expand slightly on heating, and then the displacement meter starts to go down as result of sinter softening. The measurement was stopped when the reading of the displacement meter reaches maximum (10 mm) corresponding to 30% reduction of the sinter height or the furnace temperature reached 1200 °C. A computer system with a data logger was used to simultaneously record the displacement and temperature readings throughout the tests through the thermocouple and the displacement meter.

From the data collected a softening curve can be drawn by plotting the displacement versus temperature. Typical examples of the results of the sinter softening test carried out on the samples obtained from the same batch are presented in Figure 8 for lead sinter and Figure 9 for zinc sinter. Several measurements (up to 7) were conducted for each sinter. The difference in the softening-behavior within the same sinter reflects the inherent variation of the sinter samples.

Ideally a sinter is softening when certain proportion of liquid is formed and softening curve should be smooth. However, the softening curves shown in Figures 8 and 9 do not have the same behavior. In addition to the idea softening curve some of lead sinters could show several steps softening (Figure 8). This may be caused by a few reasons: 1) sinter is porous material. If the displacement meter falls into the pore a false contraction can be shown; 2) lead sinter is not uniform in composition. Some low melting temperature materials such as lead metal, sulphide and sulphate can melt locally at relative lower temperature. Sinter lump itself does not softening but softening occurs locally; 3) lead sinter varies in structure and composition from area to area.

Initial softening has been observed to occur at as low as 700 °C in some lead sinter samples. Final softening temperatures, the temperatures at which complete collapse of the sample under

load takes place, were found to be in the range of 800-1100 °C for the lead sinters. Several separate measurements were conducted for each sinter material, and it is clear that there is some inherent variation in the behavior of the samples from the same sinter. It can be seen from Figure 8 that sudden partial collapse of the sinters occurs in some of the samples as the probe penetrates the sample. Examination of these samples has shown that samples having small variations in softening temperature have more uniform microstructure. Samples having a large variation in softening temperature, and which exhibited frequent and random collapse with temperature, have uneven microstructures. These local differences in the sinter structure in the form of changes in the phases present, and the proportions of phases, are the result of local compositional variations. These variations in turn lead to differences in the softening and melting temperatures, and the apparent viscosities of the materials.

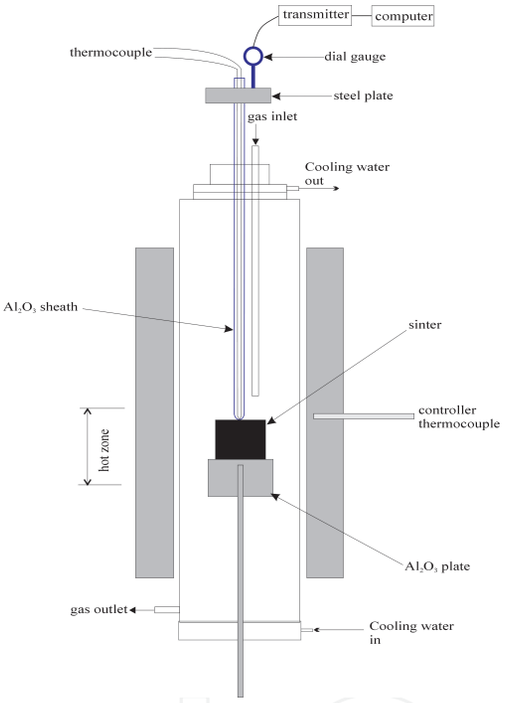

Figure 7. Apparatus used for softening temperature test [2]

ISF sinters have relative uniform composition and structure within a batch of sample. The softening curves for a given ISF sinter do not variation as great as the lead sinter shown in Figure 8. The softening curves shown in Figure 9 are from different sinter samples and they can be described as three typical types. Type 1 (G3 in Figure 9) shows a softening curve in which the sinter softening starts at approximately 950 ºC and the displacement reaches 5 mm at 1140 ºC. Type 2 (M3 in Figure 9) shows a softening curve in which the sinter softens very slow. Although the softening started at 1050 ºC, this was not great, and the sample still retained its strength at temperature. Because the softening test stopped at 1200 ºC it was difficult to obtain a temperature in which the displacement drops dramatically. Type 3 is the common softening curve observed in most of the ISF sinters and their softening behaviors are between

http://dx.doi.org/10.5772/54618

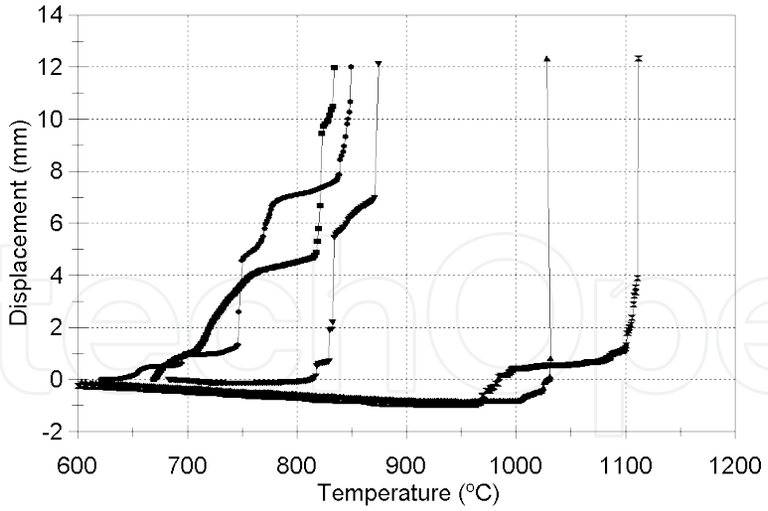

(heating rate 400 °C/hour, load 235g and 8 mm diameter sheath)

Figure 8. Softening Curves of a Typical Lead Sinter in Air [13]

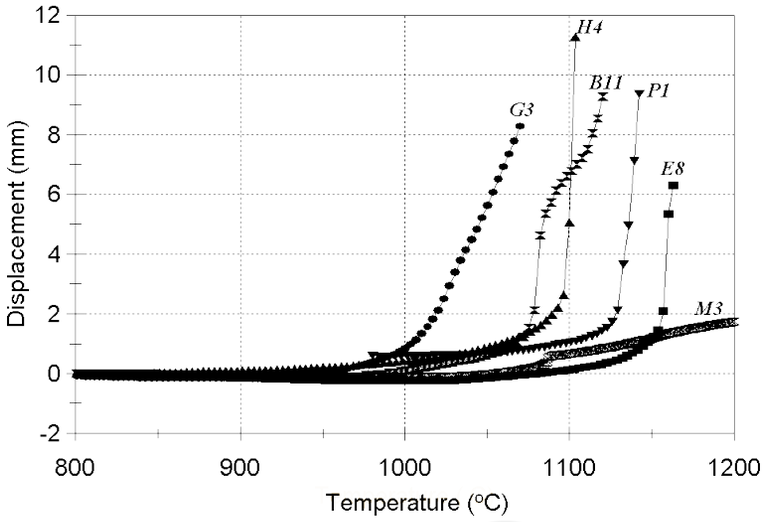

(heating rate 400 °C/hour, load 400g and 8 mm diameter sheath)

Figure 9. Typical softening curves of ISF sinters in air [2]

Type 1 and Type 2. Examination of the ISF sinters shows that the sample G3 has the microstructure shown in Figure 6b which contains the highest proportion of glass phase and low aspect ratio zincite. In contrast, the sample M3 has the microstructure shown in Figure 6a which contains the lowest proportion of glass phase and high aspect ratio zincite. Other samples such as B11, E8, H4 and P1 have the microstructures shown in Figures 6c and 6d. In brief, it can be explained that the softening in Type 1 mainly depends on the proportion of the liquid phase formed. The softening in Type 2 mainly depends on the zincite framework present in the sample. The softening in Type 3 depends on both of the proportion of the liquid phase and zincite framework.

2.2. Factors to determine the sinter quality

During the oxidative sintering of zinc sulphide concentrates in the sinter machine, and the reduction of sinter in the blast furnace t, the sinter is subjected to load from the overlying burden. Crucial to the operation and high productivity of both sintering and reduction processes is the ability to maintain bed high bed voidage, thus providing low resistance to gas flow.

Previous studies [4-5] have shown that the ISF sinter softening characteristics at temperature are related to bulk composition and microstructure of the sinter. It was found that sinters containing a high proportion of connected glass phase exhibited low softening temperatures. High softening temperature sinter is always associated with formation of microstructures containing high aspect ratio crystals of refractory zincite (ZnO), which at high proportions of this phase can give rise to a 3D interlocking network structure. Pure ZnO is known to have a melting temperature of 1975 ºC [6], far in excess of the silicate matrix. Although a number of microstructural types of the ISF sinter were identified in these earlier studies [4-5], to date no quantitative relationships between bulk composition and softening temperature are available to assist in the design of sinter materials.

Recent research by the authors [7] using synthetic sinter (PbO-ZnO-Fe_2O_3-CaO-SiO_2-Al_2O_3) materials has shown that the microstructures produced in air depend principally on the bulk composition and temperature. The aspect ratio of the zincite present in these sinters was found to increase with increasing peak bed temperature and increasing CaO/SiO_2 ratio. The relationships between high temperature softening behaviour and material microstructure in these synthetic materials is systematically investigated and compared to the results obtained from industrial sinters.

The synthetic sinters samples used for softening temperature tests were prepared from mixtures of pure oxide powders. The details of preparation and compositions of these synthetic materials are given in a previous publication by the authors [7]. The synthetic materials selected for the softening tests all contained fixed (ZnO+PbO) = 76.2% , PbO/ZnO = 0.40 by weight, having selected % Fe_2O_3 and CaO/SiO_2 ratios. The bulk compositions of the various materials, labeled as the ZM series, are summarized in Table 3.

	Bulk wt% Fe_2O_3		
CaO/SiO_2	10	14	18
0.35	ZM1	ZM6	ZM11
0.93	ZM3	ZM8	ZM13
1.5	ZM5	ZM10	ZM15

((ZnO+PbO) = 76.2%, PbO/ZnO = 0.40 by weight)

Table 3. Summary of synthetic materials used in softening tests in the present study

http://dx.doi.org/10.5772/54618

To prepare these materials water was added to each batch of approximately 50g of oxide powder mixture, the material was then shaped to a 30 mm diameter and 30 mm height cylinder. The sample was dried at 120 ºC and placed in a castable alumina plate. The sample was heated at 900 ºC for 120 minutes, and then at 1250 ºC for 30 minutes in air. After heat treatment the sample was cooled to room temperature in air in readiness for the softening temperature test. Typical microstructures of these materials are illustrated in Figure 10 [7]. The glass phase (light grey) and zincite (grey oval- shaped to plate-like) crystals are present in all samples; the angular (dark grey) phase is spinel which is only present in some of the samples.

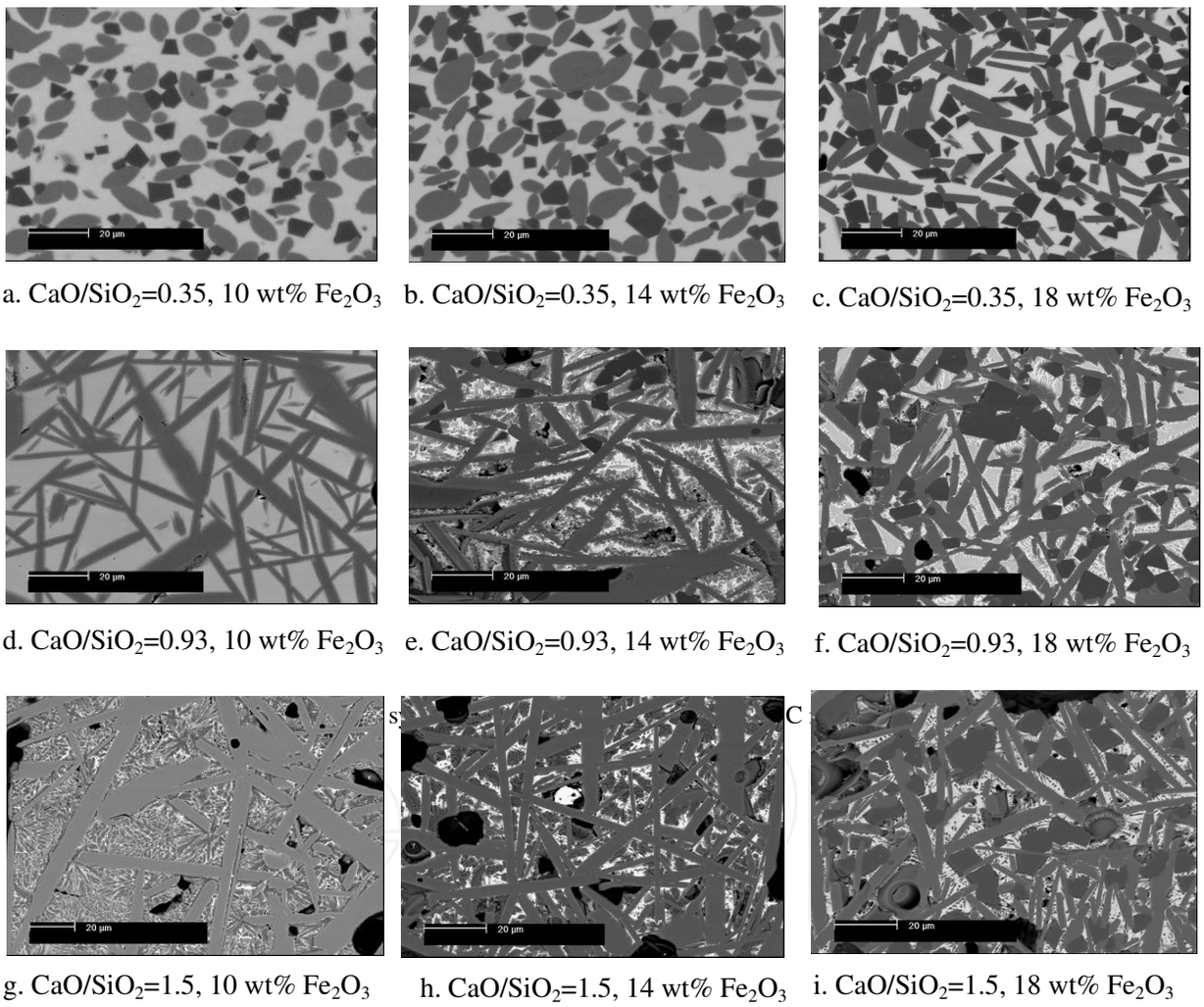

Figure 10. Typical microstructures of synthetic sinters quenched from 1250 ºC in air, scale bar 20 µm [2]

Industrial sinter feed materials and final sinter product samples have also been obtained from operational ISF plants [7-8]. Representative samples were selected from the industrial sinter lumps for examination and testing.

2.2.1. Softening temperature measurement in air

The sinter softening test used was designed to reproduce conditions that may be experienced by individual sinter samples in sintering or packed bed reactors; the test involves applying a fixed load to 30x30mm cylinders of individual sinter samples and measurement of the displacement as function of time and temperature. The tests are intended to provide information on the comparative behaviours of the materials rather than to obtain absolute measures of mechanical properties.

The softening temperatures of individual sinter lumps selected from the bulk samples were measured using the apparatus shown schematically in Figure 7. A typical example of the softening curve of sample sinter is given in Figure 11. A positive displacement reflects a softening of the sinter. The sinters initially expand slightly with increasing temperature from room temperature, then softening and contraction of the sample occurs.

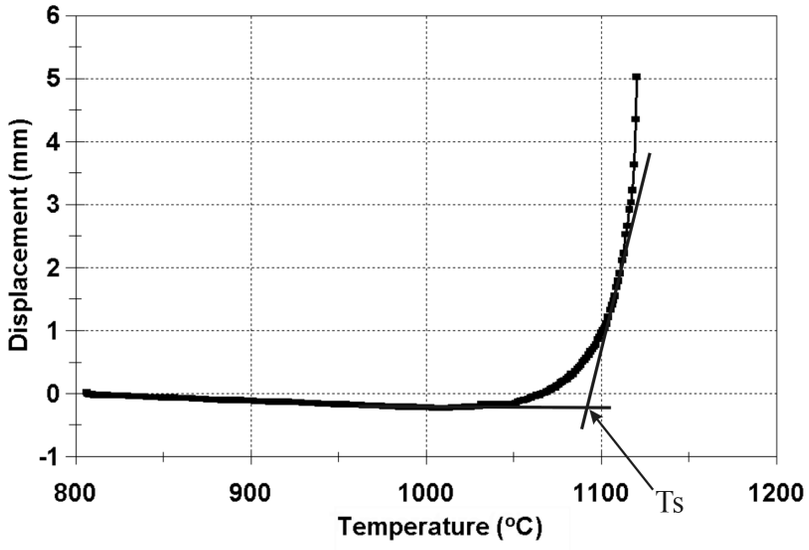

Figure 11. A typical softening curve of the synthetic ISF sinter [2]

The initial softening temperature T_s can be defined in a number of ways. In the present study it is defined by selecting an arbitrary value of displacement at a given temperature, from the intersection of the limiting lines describing expansion and contraction of the sample or the change in slope of the displacement vs temperature curve from –ve to +ve. In the case of

synthetic and industrial sinters there is no sharp transition from one behaviour to the other, there is always some uncertainty in defining the softening temperature since the value is dependant on the shape of the displacement vs temperature curve.

2.2.2. Phase Assemblages at high temperature

Assuming chemical equilibrium is achieved during softening the phases present in the synthetic sinter, their proportions and compositions can be predicted as a function of temperature and bulk composition. Calculations of the phase assemblages for the samples used in the present study are shown in Figures 12 to 20. These predictions were made using FactSage databases and computer package [9]. The volume fractions were calculated using the densities of each of the component with the following assumptions:

1. Partial molar volumes of each component in the sinter are the same as for pure liquid component;
2. No thermal expansion is taken into account; and
3. Partial molar volume of liquid component is the same as for solid component.

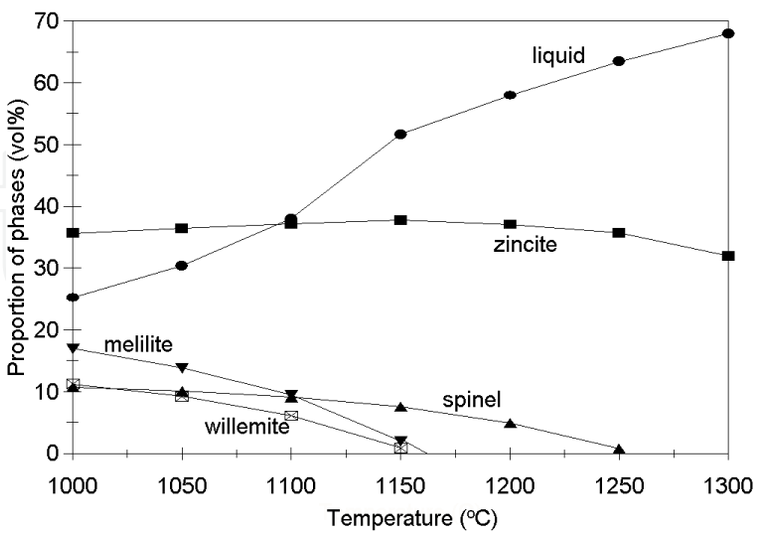

Figure 12. Proportions of phases for ZM1 calculated by FactSage in air [2]

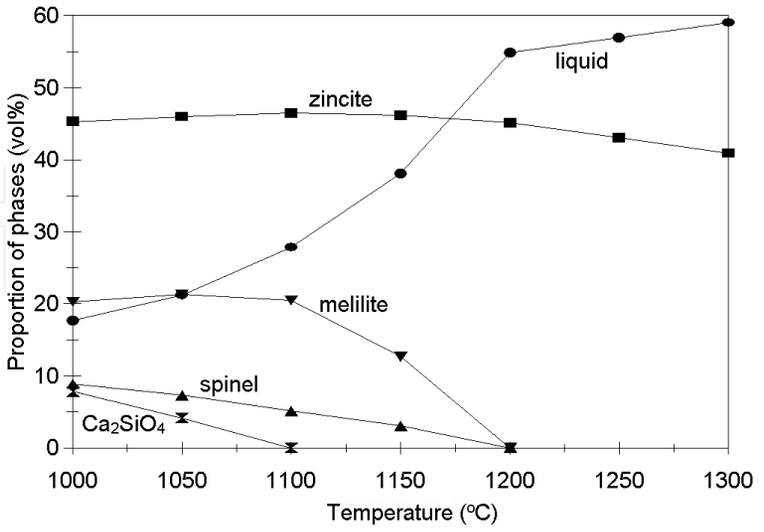

Figure 13. Proportions of phases for ZM3 calculated by FactSage in air [2]

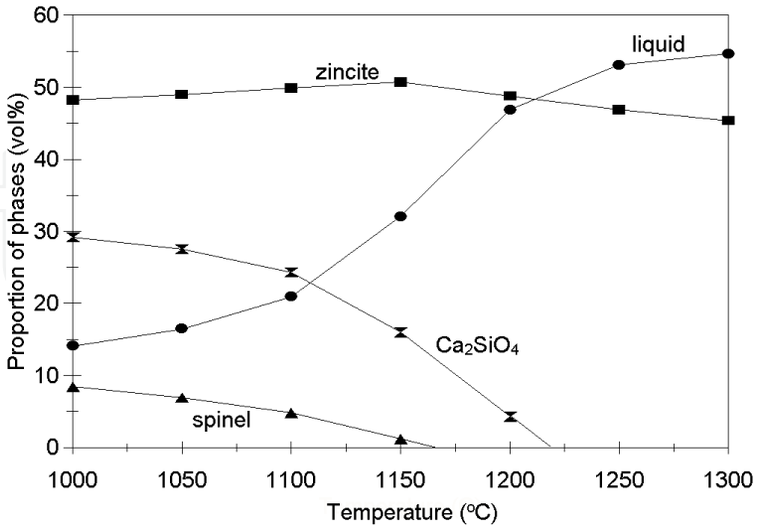

Figure 14. Proportions of phases for ZM5 calculated by FactSage in air [2]

http://dx.doi.org/10.5772/54618

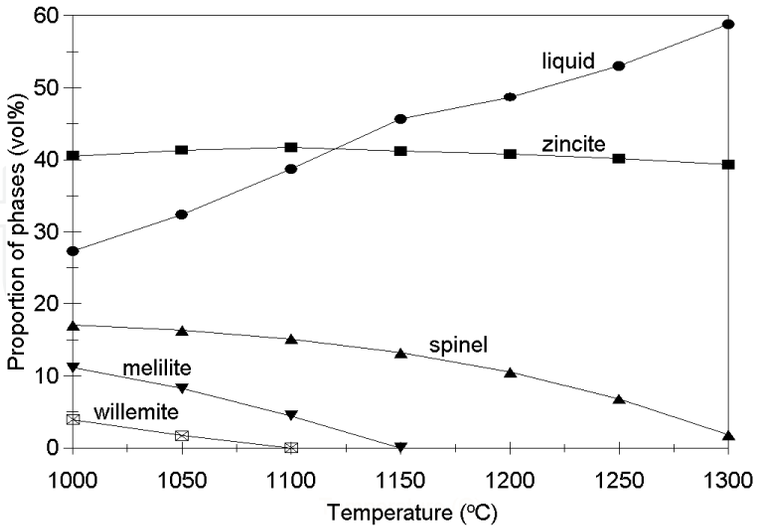

Figure 15. Proportions of phases for ZM6 calculated by FactSage in air [2]

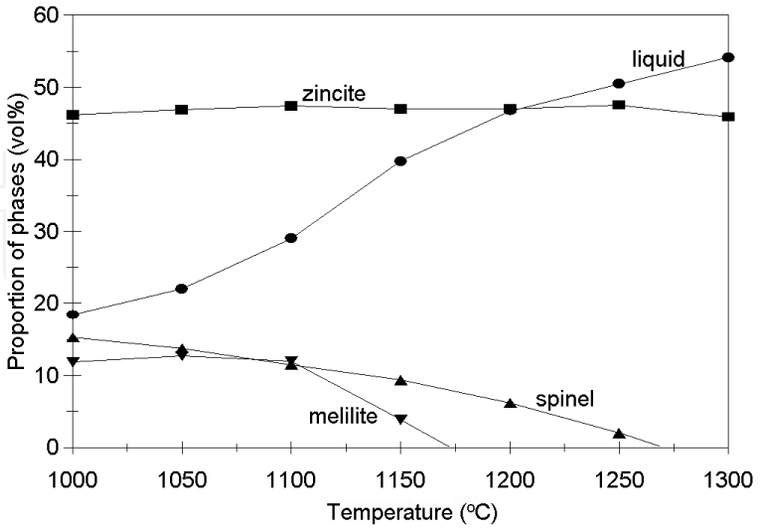

Figure 16. Proportions of phases for ZM8 calculated by FactSage in air [2]

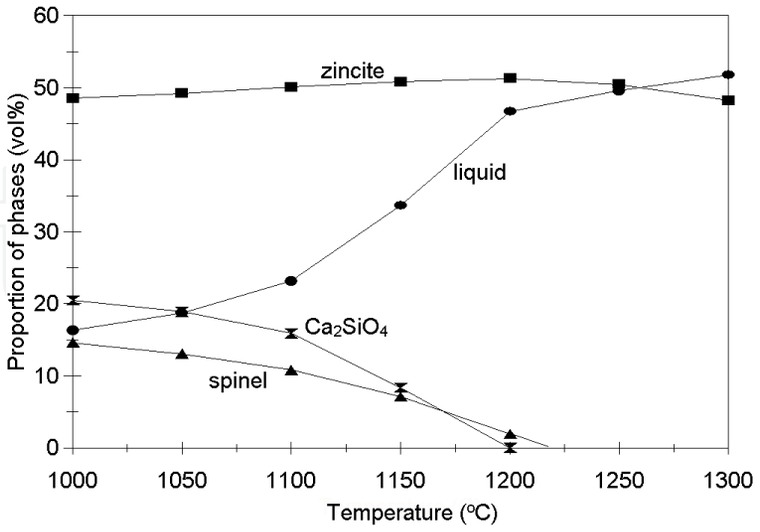

Figure 17. Proportions of phases for ZM10 calculated by FactSage in air [2]

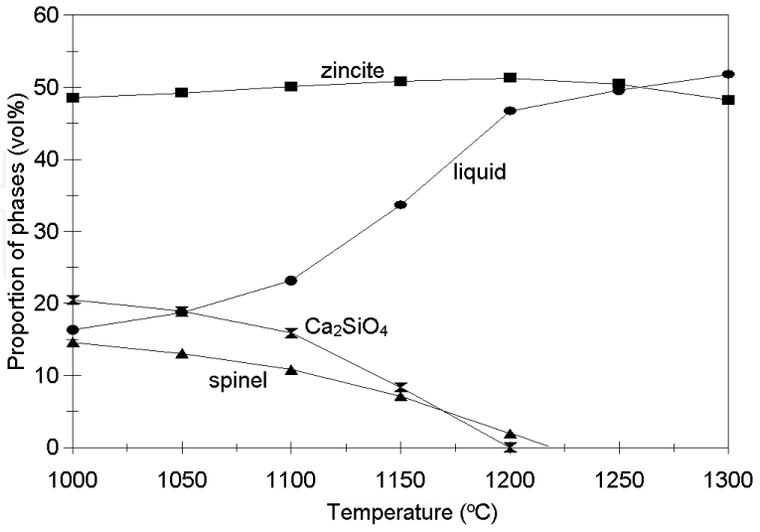

Figure 18. Proportions of phases for ZM11 calculated by FactSage in air [2]

http://dx.doi.org/10.5772/54618

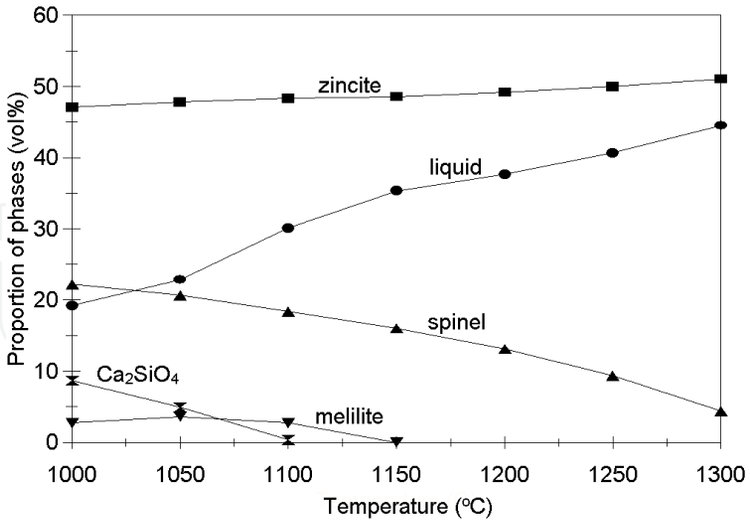

Figure 19. Proportions of phases for ZM13 calculated by FactSage in air [2]

It can be seen from Figures 12 to 19 that the three phases that are present in all samples are liquid, zincite solid solution (Zn,Fe)O, and spinel solid solution (Zn,Fe)O.Fe_2O_3. The volume of zincite phase remains almost constant over the temperature range 900-1200 °C; all samples apart from ZM1 contain 40-50 vol% zincite, ZM1 contains approximately 35 vol% zincite. All samples apart from ZM1 contain liquid phase as low as 900 °C, liquid in ZM1 appears above 950 °C. The proportion of liquid phase present increases with increasing temperature; the extent of the change in the proportion of liquid is dependent on the bulk composition of the samples. In general the % liquid at any temperature decreases with increasing CaO/SiO_2 ratio; the % spinel increases with increasing % Fe_2O_3.

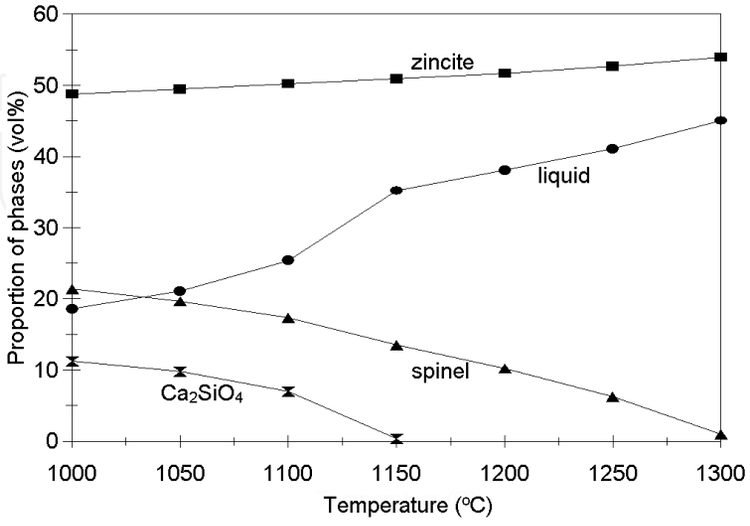

Figure 20. Proportions of phases for ZM15 calculated by FactSage in air [2]

2.2.3. Softening Temperatures of Synthetic Sinters in Air

The effects of CaO/SiO_2 ratio, "Fe_2O_3" concentration, and preparation temperature, on the softening characteristics of synthetic sinters in air are discussed in the following section.

Effect of CaO/SiO_2 ratio

Figures 21 and 22 show the effect of bulk CaO/SiO_2 ratio on the softening behaviour of the synthetic sinters containing 14 (ZM6, ZM8, ZM10) and 18 wt% "Fe_2O_3" (ZM11, ZM13, ZM15) in bulk sinter respectively. It can be seen that for both sets of data the initial softening temperatures, T_s, as given by the change in slope of the displacement vs temperature curves, increase with increasing CaO/SiO_2. For ZM6, ZM8 and ZM10 T_s is 1100, 1160 and 1180 °C respectively; at these temperatures the predicted % liquids are 38, 42 and 44 vol% respectively. For ZM11, ZM13 and ZM15 T_s is 1050, 1100 and 1160 °C respectively; at these temperatures the predicted % liquids are 30, 36 and 36 vol% respectively. Note in general that increasing CaO/SiO_2 ratio decreases the % liquid present in the sinters for given % Fe_2O_3.

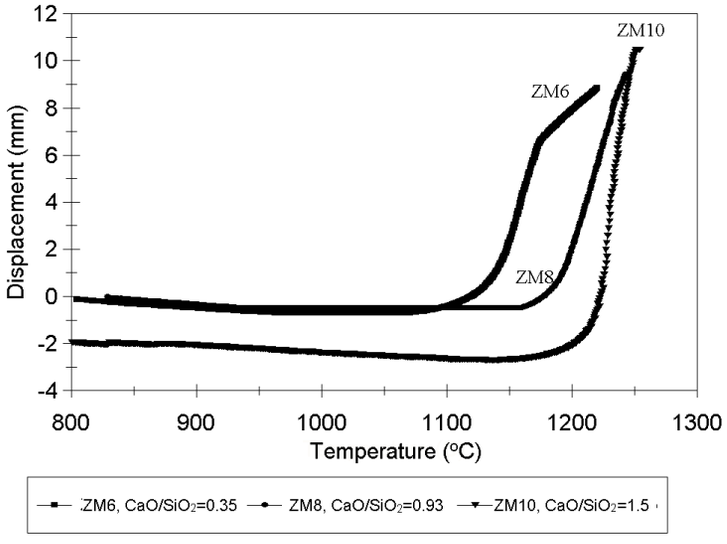

Figure 21. Effect of CaO/SiO_2 ratio on softening temperature in air at fixed 14 wt% Fe_2O_3 and PbO/ZnO=0.40 [2]

In addition the extent of softening, i.e. the positive displacement, at any temperature decreases with increasing CaO/SiO_2 ratio from 0.35 to 1.5.

Reference to the original sinter microstructures (Figure 10) shows an increase in the aspect ratio of the zincite crystals with increasing CaO/SiO_2 ratio at 1250 °C. For the samples containing 14 wt% Fe_2O_3 aspect ratios increase from 2.3 (ZM6) to 12.4 (ZM10); for 18 wt% Fe_2O_3 the aspect ratios increase from 3.6 (ZM11) to 13.3 (ZM15) with increase of CaO/SiO_2 ratio from 0.35 to 1.5.

http://dx.doi.org/10.5772/54618

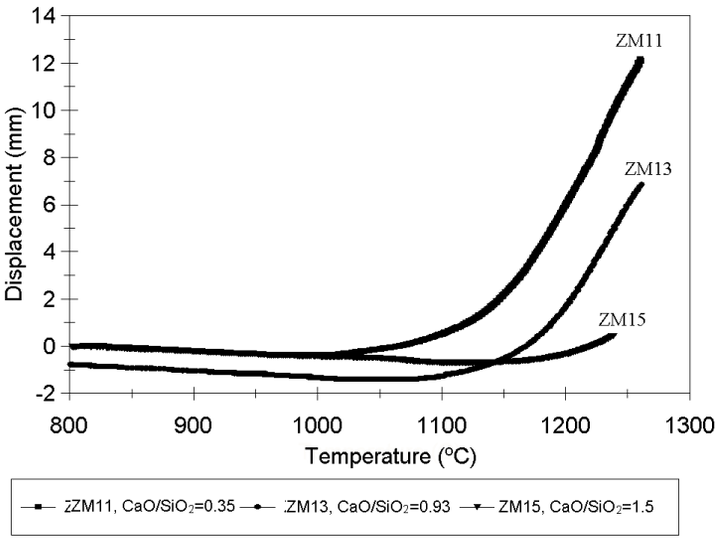

Figure 22. Effect of CaO/SiO_2 ratio on softening temperature in air at fixed 18 wt% Fe_2O_3 and PbO/ZnO=0.40 [2]

Effect of "Fe_2O_3"

It can be seen from Figure 23 samples (ZM1, ZM6 and ZM11) with CaO/SiO_2 = 0.35, having "Fe_2O_3" concentrations in bulk sinter of 10, 14 and 18 wt% respectively, have initial softening temperatures in the range 1100-1150 °C. The mean zincite crystal aspect ratios observed in these samples are in the range 2 – 4 [7], and the predicted equilibrium % liquids at 1100 °C are in the range 33-38 vol%.

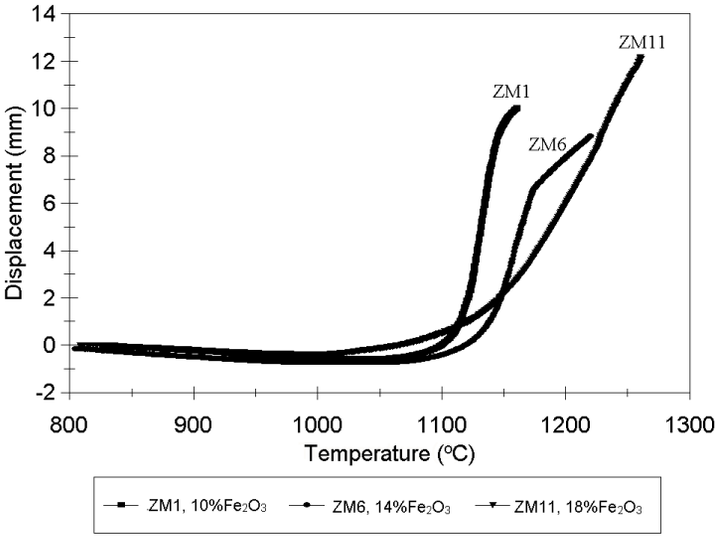

Figure 23. Effect of Fe_2O_3 concentration in sinter on softening temperature in air at fixed CaO/SiO_2 ratio of 0.35 and PbO/ZnO=0.40 [2]

It can be seen from Figure 24 samples (ZM3, ZM8, ZM13) with CaO/SiO_2 ratio of 0.93, the initial softening temperatures, appear to be the range 1150-1200 °C. The mean zincite crystal aspect ratios are in the range 9-11 [7], yet at 1150 °C the % liquid is in the range 35-40 vol%.

It can be seen from Figures 23 and 24 that at fixed CaO/SiO_2 ratio, increase of "Fe_2O_3" concentrations in bulk sinter from 10 to 18 wt% does not have significant effect on softening temperature.

Effect of preparation temperature

The effect of sinter preparation temperature on softening temperature in air is shown in Figure 25. It can be seen that for sinter ZM8 (14 wt% "Fe_2O_3", CaO/SiO_2 = 0.93 and PbO/ZnO = 0.40) the softening temperature of the sample prepared at 1300 °C in air is significantly higher than either of the samples prepared at 1200 to 1250 ºC. The softening temperatures of the samples prepared at 1200 and 1250 ºC are similar.

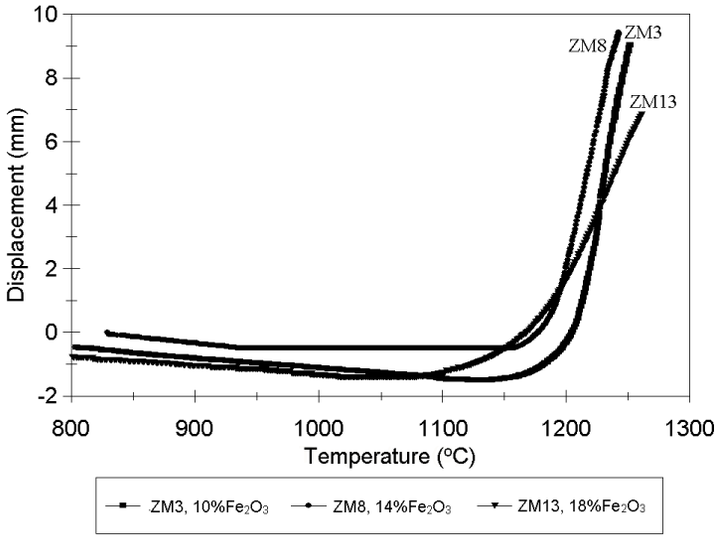

Figure 24. Effect of Fe_2O_3 concentration in sinter on softening temperature in air at fixed CaO/SiO_2 ratio of 0.93 and PbO/ZnO=0.40 [2]

Previous study [7] have shown increasing the preparation temperature for a given bulk composition results in an increase in % Fe_2O_3 dissolved in the zincite crystals and the corresponding increase in aspect ratio of the crystals. For a given volume fraction of zincite increased aspect ratio leads to increased framework formation.

All of the softening tests undertaken show consistent trends between microstructure and the extent of softening of the sample at a given temperature; increased zincite aspect ratio leads to increased resistance to deformation at temperature.

http://dx.doi.org/10.5772/54618

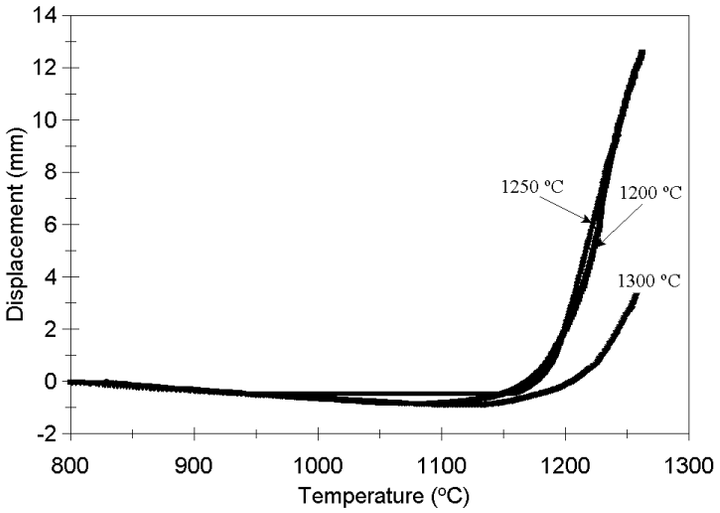

Figure 25. Effect of treatment temperature on softening temperature in air for sinter ZM8 (14 wt% Fe_2O_3, CaO/SiO_2=0.93 and PbO/ZnO=0.40) [2]

2.3. Conceptual sinter softening model

To assist in the understanding and analysis of the results obtained in the present and previous test work a conceptual sinter softening model is developed.

It is well established that the strength of a composite material is dependent on the physical properties of the phases present, the volume fractions of the phases and the macro- and micro-structure of the composite. The application of any stress, compressive or shear, to a liquid phase will result in viscous flow of this phase. Crystalline solid materials in contrast are rigid and behave elastically at low stress, permanent or plastic deformation, or fracture requires that a critical yield or fracture stress be exceeded [10].

The mechanical properties of a composite materials consisting of an isolated solid phase completely surrounded by a high volume fraction of second liquid or partially liquid phase matrix (see Figure 26) will largely be dependent on the properties of this matrix material. In this limiting condition at room temperature the matrix material is rigid, being in the form of crystalline or amorphous solid. If the matrix consists of a single crystalline solid phase, as the sample is heated this material becomes fully liquid at a given temperature. If the matrix material consists of a glass, on heating the glassy matrix reaches its glass transition temperature T_g, the glass then becomes liquid and the matrix material loses its compressive strength and begins to flow. With increasing temperature the viscosity of, for example, a high–PbO liquid silicate such as encountered in the samples studied in the present investigation, decreases and the deformation rate increases; since the material behaviour is determined by the properties of the liquid phase complete collapse of the sample under load occurs. In the limiting case for the formation of low viscosity liquid matrix at a given temperature the matrix phase loses its compressive strength and the structure will completely collapse, resulting in a step change in deformation at that temperature; the maximum compression of the sample C_{max} = 100%. This

material behaviour is exemplified by sample ZM1, which consists of isolated zincite and spinel crystals surrounded at room temperature by a glassy matrix (Figure 10a)

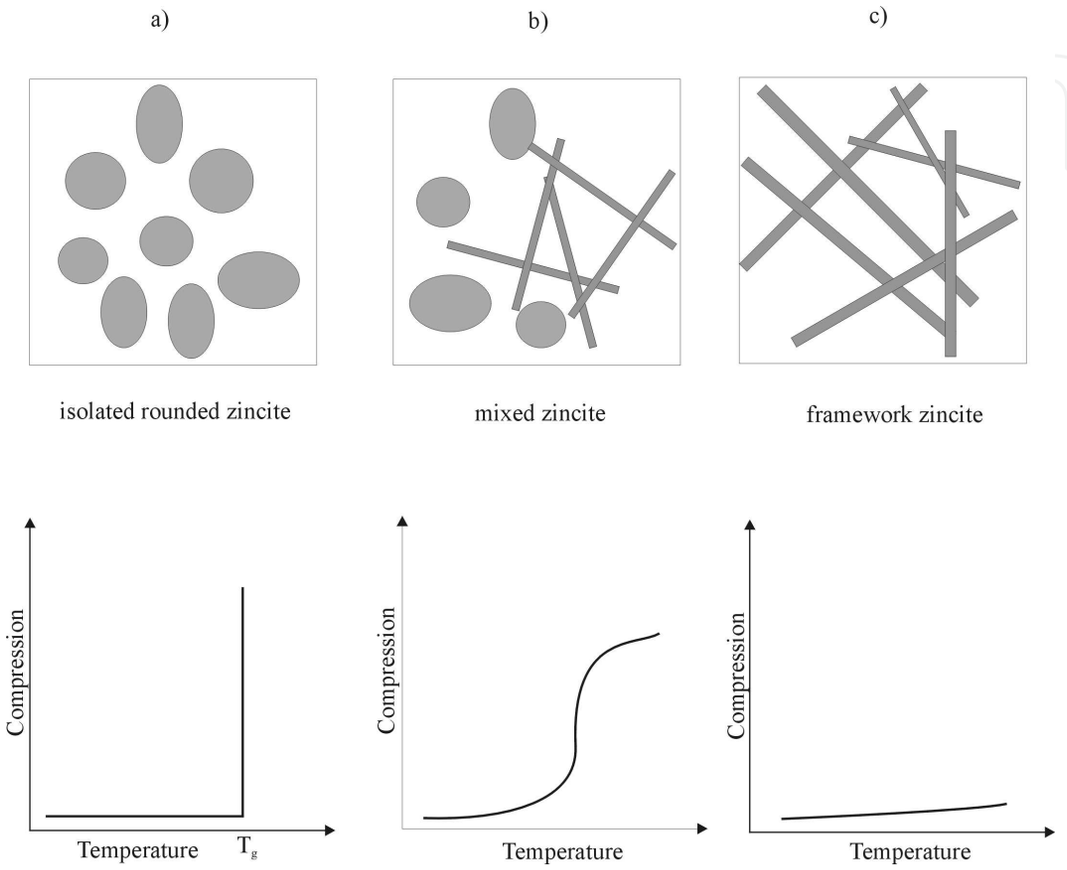

Figure 26. Idealised sinter softening model [2]

In contrast if the composite consists of a rigid 3-dimensional framework structure of a high melting temperature solid material the deformation characteristics of the composite material will not change when the matrix material becomes molten, since the material will be fully supported by the rigid 3D framework. In this case there is no compression of the material, i.e. $C_{max} = 0$, as the temperature is increased through and beyond the melting temperature of the matrix (see Figure 1d). On this basis the higher the proportion of framework zincite present in the material the lower the maximum compression of the sinter, C_{max}.

In the case of the synthetic sinters under study there are ranges of microstructure types, and melting occurs over a range of temperatures. Nevertheless this simplified analysis of sinter softening process indicates that two measures should be used to characterise sinter softening behaviour,

i. Ts, initial softening temperature microstructures, which is determined primarily by the strength of the matrix material, and

http://dx.doi.org/10.5772/54618

ii. The proportion of framework zincite present in the material, which determines C_{max}, the maximum deformation and the deformation rate of the sinter at any temperature.

The measured softening curves for typical synthetic ISF sinters are presented in Figures 21-25. Comparison with the calculated phases fractions from Figures 12 to 20 shows that the initial softening temperatures T_s in all cases corresponds to the temperature with 35-50 volume pct of liquid phase. Based on purely geometric considerations this would correspond to the minimum volume required to form a continuous liquid phase between the randomly distributed solid phases present in the individual samples.

The extent of formation of the framework zincite in the structures will depend on the volume fraction of zincite phase and the aspect ratio of these crystals. The thermodynamic analysis indicates that all synthetic sinter samples contain approximately 40-50 vol% zincite over the temperature range 900-1300 °C; this variation is insufficient on its own to explain the differences in softening behavior of the materials.

It has been well established [7] that the aspect ratio of the zincite can change significantly with bulk composition and thermal history. The softening tests carried out in the present study indicate displacement as a function of temperature for a given applied stress and heating rate (400 °C/h). The displacement vs temperature plots may also be interpreted as displacement vs time. The slopes of these softening curves reflect the strain rate at constant stress. It can be seen from the data shown in Figures 21 to 25 that, within experimental uncertainty, there are general trends in behavior with decreasing strain rate obtained with increasing zincite aspect ratio, increasing CaO/SiO_2 ratio, and increasing bulk iron concentration.

It appears that even though complete 3-D networks of zincite are not formed in all cases the increased aspect ratio of the zincite increases the resistance to deformation under load, i.e. increases the effective viscosities of these composite materials.

2.3.1. Implications for industrial practice

The results obtained from the present study are consistent with softening temperature measurements and microstructural analysis carried out on industrial ISF sinters [8]. Examples of the different softening behaviours observed for ISF sinters have been shown in Figure 9. It can be seen that initial softening of sample G3 starts at approximately 950 °C and collapses of the structure is complete over a relatively narrow range of temperatures. In contrast, although the softening of the sinter M3 starts at approximately 1050 °C but retains its strength at temperature until at least 1200 ºC. This contrasting behaviour is reflected in the very different microstructures observed in these samples [7]; G3 contains isolated zincite crystals of low aspect ratio (2-3), whereas M3 consists almost entirely of high aspect ratio zincite that forms an interlocking 3-D network of refractory material (aspect ratio >10). The CaO/SiO_2 ratios are 0.80 for G3 and 1.14 for M3 respectively.

Most ISF sinters have softening characterisics that are between these two extremes; the microstructure of these materials show this contain both isolated zincite and zincite having a range of aspect ratios. This is demonstrated in sinter B11 [7].

In developing an understanding of the structural factors influencing the strength of sinters these have to be considered at Macro-, Meso-, and Micro-structural levels. The product sinter consists of partially fused granules of oxidised zinc concentrates and flux materials. The porosity of the sinter depends on the degree of fusion of the granules. The porosity and density of the ISF sinter lumps were measured using an Australian Standard AS 4133.2.1.2-1993 "Rock porosity and density test-Determination of rock porosity and dry density-Saturation and buoyancy techniques". It was found that industrial ISF sinters have typical porosities in the range 25-40%. The sinter materials experience differences in thermal history during the sintering process due to differences gas flow path and combustion within the ignition, heating and sintering layers of the bed; these result in *macro-structural* differences over the range (10 – 100mm).

In the ISF sintering process approximately 65-75% by weight of the sinter is recycled. The product sinter is crushed, separated by size with lump sinter 100-200mm diameter sent to the ISF; the remainder is further crushed, sized and returned to the feed preparation. This recycled or "return" material is coated with fresh concentrate to form approximately spherical feed granules to the sinter process. These feed granules consist of individual return particles or and composites, agglomerates consisting of a number of coated return particles. *Meso-structural* differences in the range (1–10mm) are the result of gross differences in composition at granule level due to differences in thermal history arising from; local variations in the proportions of returns/fresh feed; single particle granule or composite granules, incomplete oxidation of sulphides, incomplete dissolution of fluxes e.g. CaO, or recycled materials, e.g. slag.

Microstructural differences in the range (10-100μm) reflect differences in crystal shape, phases formed, proportion of phases, and are typically the result of local compositional variation, cooling rate/crystallisation.

Trailing thermocouple tests on ISF sinter plants [11-12] have shown that although sulphur elimination is largely achieved because of the low peak bed temperatures, strong fusion of the granules does not occur in the bottom third of the updraft sinter bed. It has also been shown [7,11] that, far from helping to strengthen the structure, reheating the framework zincite structure at these low temperatures leads to the breakdown of the interlocking plates and reduction in zincite aspect ratio.

The top part of the sintering layer achieves the highest peak bed temperature, since the gas is preheated before it reaches the combustion zone. It is in this zone that is to be expected that most material is converted to high aspect ratio zincite.

Important factors that assist in achieving high peak bed temperatures include

- Fuel loading
- Feed ignition temperature
- Moisture content
- Feed granule size distribution

http://dx.doi.org/10.5772/54618

- Blowing rate and profile

Examination of the feed characteristics of all industrial sinters tested shows that significantly the sinter M3, which consistently contain high % framework structure, were produced from feed materials with small mean size (4mm) and narrow size distribution (σ_{size} = 5mm). Small granule diameter favours thinner fresh sulphide feed layer thickness on the granules because of the high surface area. Combustion of fresh feed is therefore more likely to take place rapidly. The smaller granule size also means that heat transfer to the return material at the core of the granules is rapid; this ensures that the return material is heated to a high peak bed temperature and not degraded by reheating to temperatures below the optimum value.

2.4. How to make high quality sinter

An extensive program of experimental and modeling studies has been carried out to improve the understanding of the factors affecting the quality of lead blast furnace sinter and lead smelting slag, and to develop methods used to characterise these materials, with a view to improving plant operations. [13] The program includes the collection of sinter samples and plant information from four different lead sinter plants, the characterization of these sinter samples and samples from subsequent plant trials, consultation with plant engineers and laboratory-based studies at the University of Queensland.

As part of the research program plant trials have been undertaken at Mount Isa lead sinter plant. In the Mount Isa Mines lead smelter of Xstrata Zinc, an updraught lead sinter machine is used to prepare feedstock for the lead blast furnace. [14] The aims of the process are to

a. produce self-fluxing lump material that maximises blast furnace productivity, and

b. remove excess sulphur from the charge.

The process combines fine particulate materials sourced from metal concentrates, recycled materials and fluxes, into lump material that is physically strong, both at ambient temperatures and within the blast furnace, and, chemically reactive in the blast furnace so that metal values can be recovered.

To incorporate all feed materials into the sinter and to form a uniform strong structure it is important to obtain high peak bed temperature during sintering process. [5,11,15] The sintering temperature has been shown to be related to a number of factors, including fuel content, composition, size distribution and moisture of the sinter feed.[[12,15-16] The gas temperature above the sinter bed is usually used as an indication of the sintering temperature, or a heat balance can be performed to predict the sintering temperature. Since the lead sinter machine is a closed and moving system it is very difficult to use conventional trailing thermocouples to measure the temperature profile within the sinter bed.

The aim of this study is to determine the temperature profile during sintering and the effect of thermal history on the sinter properties. This is achieved through the use of a wireless temperature probe developed at the University of Queensland, metallographic studies of product sinters and measurement of sinter softening characteristics.

2.4.1. Sintering temperature measurement

Lead sinter plant trials have been carried out at the Xstrata Zinc sinter plant (Mount Isa) by the author and Xstrata Zinc staff. The design of the hood at the Mount Isa sinter plant is such that there is a 10 cm gap between the ventilation hoods for the main feed hopper and the sinter machine. This space is sufficient for thermocouples to be inserted through the side wall of the sinter pallet after the main layer of sinter feed material was charged onto the sinter machine. The thermocouple once in place progresses through the length of the sinter bed and is discharged with the sinter lump. A wireless temperature probe was used to measure the temperature within the sinter bed. A K-type thermocouple was inserted into the sinter bed and connected to a radio transmitter, which is attached to the outside of the pallet and moves with the sinter bed as shown in Figure 27. A radio receiver remote from the sinter machine is connected to a computer. The temperature measured by the thermocouple inside the sinter bed is converted to the radio signal by the transmitter. The receiver outside then converts the radio signals to digital output, which is recorded on a computer.

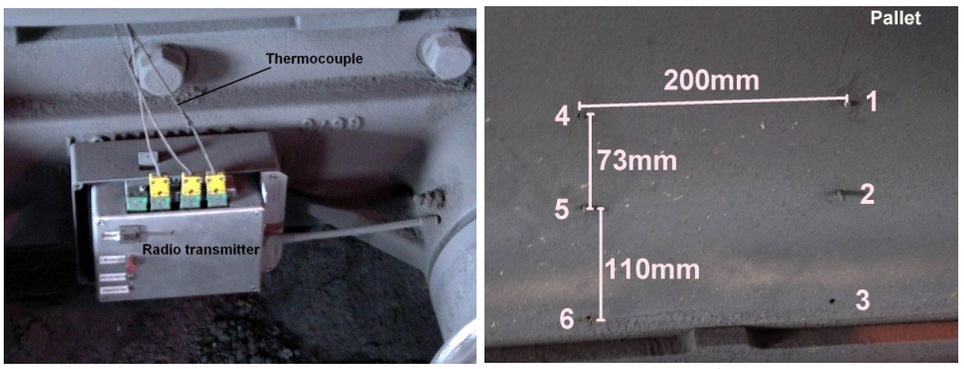

(a) (b)

Figure 27. The radio transmitter fixed on the pallet and positions of holes on side of the pallet at Mount Isa lead sinter machine [19]

Two sets trials have been conducted. The first set trials were conducted using a single channel wireless transmitter. An upgraded wireless transmitter with four channels was used in the second set trials.

The total initial sinter bed depth was 440mm. In the first set trials two holes of 5 mm diameter were drilled through the side of the sinter machine pallet. The bottom hole was made at ½ bed depth (220 mm) and the top hole was made at 2/3 bed depth (293 mm), height measured from grate surface.

In the second set trials six holes were drilled through the side of the sinter machine pallet as shown in Figure 27. The bottom holes (holes 3 and 6) are 110 mm above the sinter bed grate that are ¼ height of the initial sinter bed. The holes in the middle (2 and 5) are ½ height of the initial sinter bed and the holes in the top (1 and 4) are 2/3 height of the initial sinter bed.

The maximum working temperature of the transmitter is 50 ºC. The success of the trials indicates that the temperature on the outside of the pallet remains below 50 ºC throughout the

http://dx.doi.org/10.5772/54618

cycle. The sinter machine motion had to be briefly interrupted for the insertion of the thermocouples. Due to the time limitation for stopping the sinter machine it was only possible to insert 2 or 3 thermocouples at a time. Usually two thermocouples were used in the trials. The speeds of the sinter machine were maintained in the range of 130-140 cm/min during the first set trials and 120−130 cm/min for the second set. In both sets of the trials the sinter samples and plant operation conditions corresponding to the temperature profiles were collected.

The temperature profiles recorded during the first set trials are presented in Figure 28. It can be seen that in trials 1.1 and 1.2 peak bed temperatures in the range 1050-1080 ºC were observed. In trial 1.3 a peak bed temperature of 870 ºC was observed. In trials 1.1 and 1.2 the temperature remained above 800 ºC until the end of the sinter bed. In trial 3 the sinter bed temperature returned to ambient temperature after a period of approximately 10 minutes. The temperature profiles measured in trials 1.1 and 1.2 are most commonly observed when the thermocouple is inside the sinter lump. These temperatures represent real sintering temperature. In the case of trial 1.3 the temperature dropped rapidly after the peak temperature. This indicates that the thermocouple was most likely outside or in the void between the sinter lumps. Since these data are all taken from the same pallet but at different times it is an indicator of feed property variation within the process.

Results of the measurements during the second set trials are presented in Figure 29. In the trial 2.1 two thermocouples were inserted at 1/4 and 2/3 bed heights respectively. It can be seen that the temperature in the bottom hole rapidly increased from 100 ºC to approximately 1120 ºC and remained at the peak temperature for 10 minutes. A peak temperature of 1190 ºC in the top hole was achieved, with most of the temperature rise not occurring until after 15 minutes of travel; this is consistent with the passage of the combustion front up through bed. The peak temperature in the upper is much higher (170 ºC) than that in the lower part; again this is expected due to the preheating of the gas from the sintered charge in the lower bed.

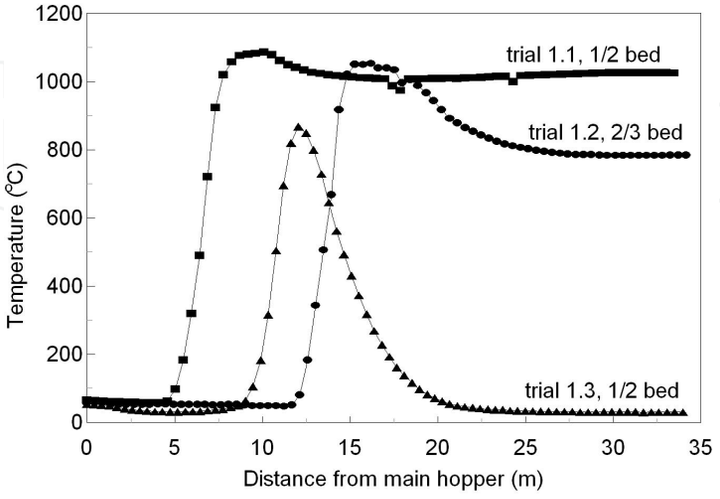

Figure 28. Bed temperature profiles against sinter pallet position at Mount Isa Mines measured during 1st set trials [19]

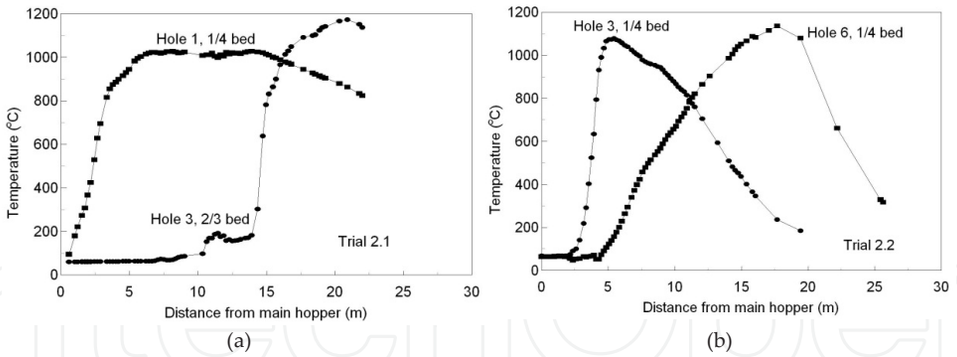

Figure 29. Temperature profiles measured during 2nd set trials [19]

In the trial 2.2 (Figure 29) two thermocouples were inserted into the pallet at the same bed height (1/4). It can be seen that the temperature in hole 3 increased rapidly to 1100 ºC and the temperature in hole 6 increased slowly to 1135 ºC. The horizontal distance between the holes are 200 mm but the peak temperatures were reached at different windbox positions. This variation of the temperature at different position of the sinter bed at the same height indicates possible differences in ignition conditions or variation in feed property along the bed.

2.4.2. Operating conditions and results of the analysis

During the plant trials, samples of the sinter machine feed and sinter lump were collected. The bulk compositions of these samples analysed by X-ray fluorescence (XRF) are given in Table 4. I1 and I5 are the sinter lump and feed collected during the first set trials and I8 and I10 are the sinter lump and feed collected during the second set trials respectively.

It can be seen from Table 4 that the fuel (sulphur) content in the sinter feeds I5 and I10 are close and the ratio of PbO/(CaO+SiO_2) in I5 (3.24) is much higher than that in I10 (2.21). The CaO/SiO_2 ratio in sinter I8 is higher than that in sinter I1. Ratio of raw feed to total feed is reported to be 0.165 in I5 and 0.175 in I10. CdO vapour pressure increases with increasing temperature; the concentration of CdO in sinter is usually used to be indication of the sintering temperature. It is seen in Table 1 that Cd contents in I8 and I10 are lower than those in I1 and I5. This confirms that the sintering temperature of I8 is higher than that of I1.

Sample	Composition (wt%)												
	Pb	Zn	Fe	CaO	SiO_2	Al_2O_3	MgO	S	Cu	Cd	As	CaO/SiO_2	PbO/(CaO+SiO_2)
I1–sinter	51.8	5.4	8.7	8.9	7.8	0.77	0.45	1.9	0.29	0.52	0.04	1.14	3.34
I5–feed	48.7	5.1	8.4	8.4	7.8	0.76	0.43	7.4	0.29	0.68	0.04	1.08	3.24
I8–sinter	45.1	6.6	10.2	10.9	8.4	0.97	0.41	1.6	0.67	0.19	0.1	1.30	2.52
I10–feed	41.4	5.9	8.4	11.1	9.1	0.87	0.36	7.1	0.56	0.31	0.05	1.22	2.21

Table 4. Bulk compositions of "as-received" sinter lump and sinter feed

http://dx.doi.org/10.5772/54618

The size analysis has been carried out for sinter machine feeds using mechanical screening. The size distributions of sinter machine feeds I5 and I10 are shown in Figure 30. At the time of 1st set trials the crusher for returned sinters was worn; this resulted in an uneven size distribution of the return sinter contained within I5. It can be seen from Figure 30 that in the sinter feed I5 the proportions of the feed smaller than 2mm and larger than 15mm are much higher than those in sinter feed I10. As a result of the bimodal size distribution the permeability of the sinter bed is low during the first set trials. This is reflected in the higher windbox air pressures of 1st set trials than that of 2nd set trials shown in Figure 31a.

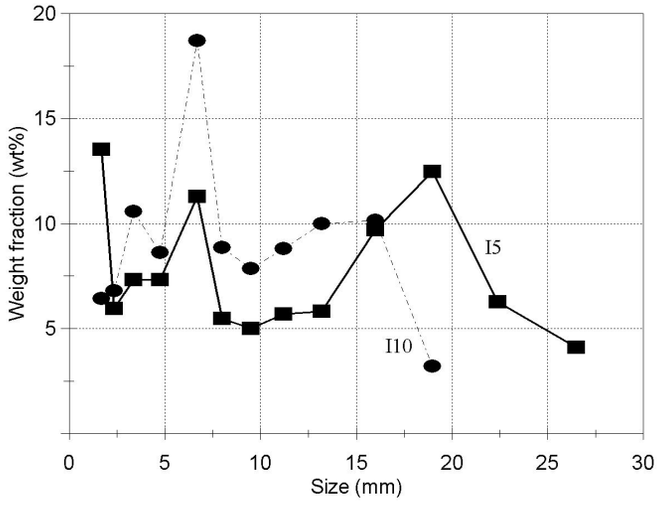

Figure 30. Size distributions of sinter feeds I5 from 1st set trials and I10 from 2nd set trials [19]

Figure 31b shows the hood temperatures measured during the two sets trials. Note that the hood thermocouple in windbox 6 was not working during the trials. It can be seen from Figure 31b that the peak hood temperature in 2nd set trials is 150 °C higher than that in 1st set trials.

Typical microstructures of sinter lump I1 and I8 are shown in Figure 32. It can be seen from the figure that plate-like melilite ($2CaO.ZnO.2SiO_2$) crystals, equiaxed crystals of spinel ($ZnO.Fe_2O_3$) and glassy lead silicate are all present in both sinters. However, the proportion of the plate-like melilite is much higher in I8 which forms an interconnected 3D network of refractory material that physically supports the structure during heating.

The softening characteristics of sinter lump have been investigated in air. Cubic sinter samples (30mm diameter) were used for softening temperature test. The tests were carried out by applying a fixed load of 235g to a 8mm OD closed-end alumina tube and a heating rate of 400 ºC per hour was used. A series of measurements have been carried out for each sinter sample. Figure 33 show the softening temperature curves for I1 and I8. It can be seen that the final softening temperatures of I1 are in the range of 920 to 1070 ºC. The wide range of softening temperatures is attributed to variations in sinter microstructure on a micro- and meso-scale, since the materials are composed of recycled (return) lump sinter coated and agglomerated with fused fresh feed. In contrast, the final softening temperatures of I8 are in the range of 1050 to 1130 ºC. The I8 sinter sample softens over a narrower temperature range and at higher

temperature than I1. Sinter softening temperature is a direct indication of the sinter quality, in particular sinter strength and uniformity of properties. The results shown in Figure 33 indicate that the sinter lump produced during 2nd set trials is better than that produced during the 1st set trials.

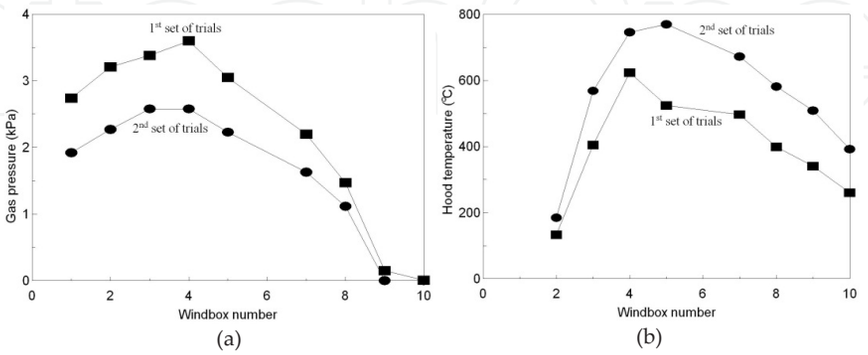

Figure 31. Gas pressures (a) and hood temperature (b) during the 1st and 2nd set trials [19]

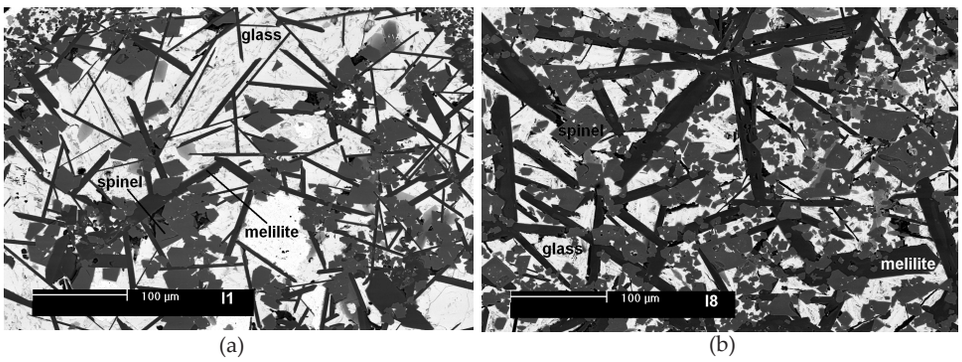

Figure 32. Typical microstructures of I1 and I8 collected during the trials [19]

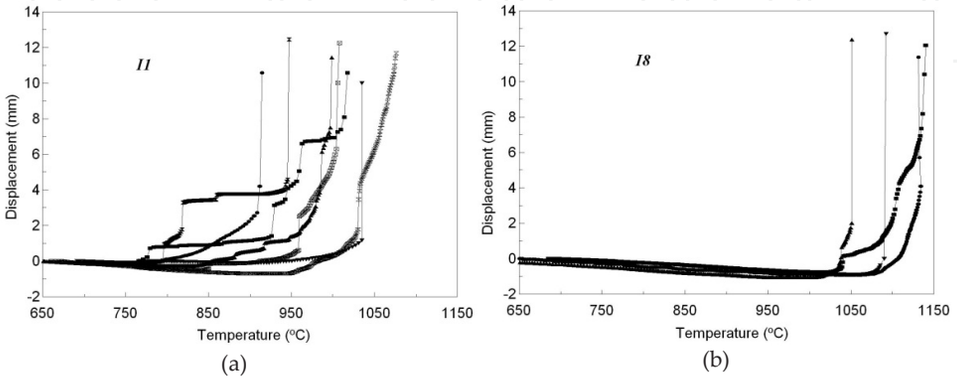

Figure 33. Softening curves of sinter lump I1 and I8 in air [19]

The predicted volume fractions of the major phases present in lead sinters I1 and I8 as a function of temperature are presented in Figure 34. It was calculated by FactSage and optimised thermodynamic database for the system $ZnO\text{-}Fe_2O_3\text{-}FeO\text{-}PbO\text{-}CaO\text{-}SiO_2$. [9,17-18] The weight fractions obtained from the calculations were converted to the volume fractions of the phases assuming: a) the partial molar volume of each component is constant and the same in the liquid and solid phases, and b) no thermal expansion takes place over the range of temperatures examined. It can be seen from Figure 34 that for both I1 and I8 the proportion of liquid phase increases with increasing temperature. The proportions of Ca_2SiO_4 and spinel decrease with increasing temperature. There is an optimum temperature range for formation of the melilite phase.

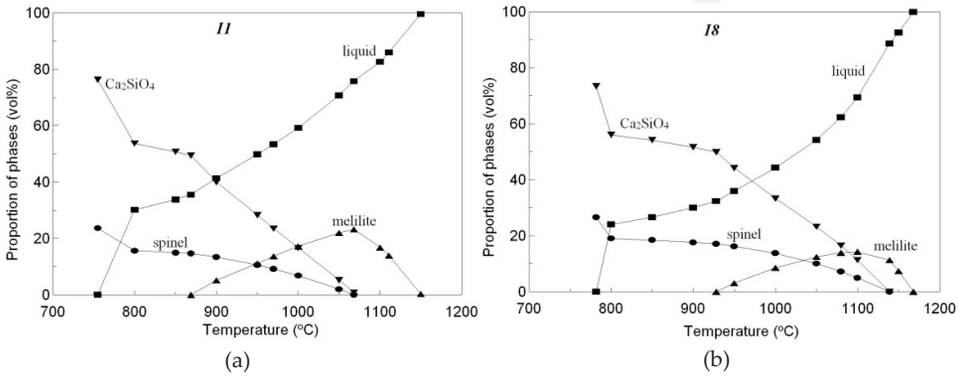

Figure 34. Phase volume fractions calculated by FactSage for as-received sinter I1and I8 [19]

2.4.3. Discussion of the correlations

The temperature profile data obtained during the plant trials can be used to correlate the attainment of peak bed temperature at a given depth in the sinter bed against the distance travelled along the sinter strand (Figure 35). The correlation assumes that the relative position of the thermocouples in the bed remained constant, i.e. the thermocouple at the ½ bed height position stays in that relative position despite the overall slumping of the sinter bed during reaction. It is known that the actual height of the sinter bed decreases as sintering proceeds; the final bed height can be 60-70% of the initial bed height.

The sinter strand is approximately 30 m long. The correlations indicate that in the case of the 1st set trials at ½ bed height the combustion front breakthrough approximately 12 m from the main hopper, allowing time for the top of the bed to cool slowly before exit from the sinter machine.

For the 2nd set trials peak bed temperatures between 1000 and 1160 ºC were achieved within the bed. The correlation between combustion front position and distance from the hopper indicates that breakthrough was only just achieved before exit from the sinter strand. The slow combustion rate achieved during the 2nd set trials compared to that for the 1st set trials.

It can be seen from the trials that there was a considerable variation in peak bed temperature and combustion front velocity, and hence significant variation in thermal history of sinter material within even a given charge of sinter material.

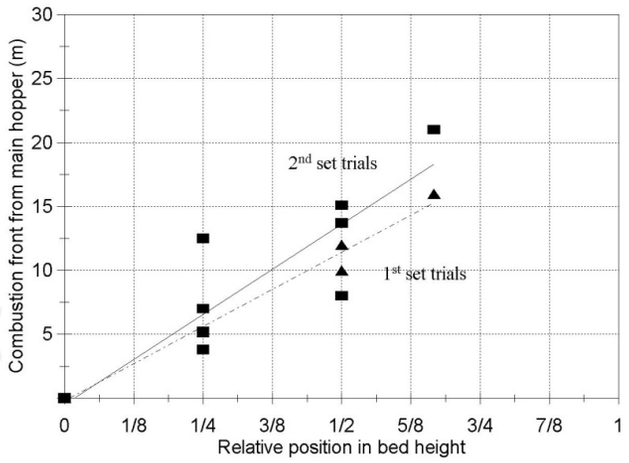

Figure 35. Correlation between combustion front and position in bed during lead sintering, initial bed height 440 mm [19]

Figure 36 shows the relationship between mean final softening temperature and peak bed temperature. It can be seen that in general the mean final softening temperature increases with increasing peak bed temperature. The average final softening temperature for the 2nd set trial sinters are 1079 ºC which is much higher than that of the 1st set trial sinters (1003 ºC).

Peak bed temperature is not monitored in everyday operation. Instead, temperature is commonly measured in the ventilation hood above the sinter strand. This is used in many plants as an indication of sinter machine performance. Relationship between peak bed temperature and peak hood temperature at Mount Isa lead sinter plant is shown in Figure 37. It can be seen that there is strong correlation between the peak bed temperature and the peak hood temperature; this indicates that the peak bed temperature in lead sinter plant can be related to the hood temperatures, the latter being available to the sinter plant operators as an on-line measurement.

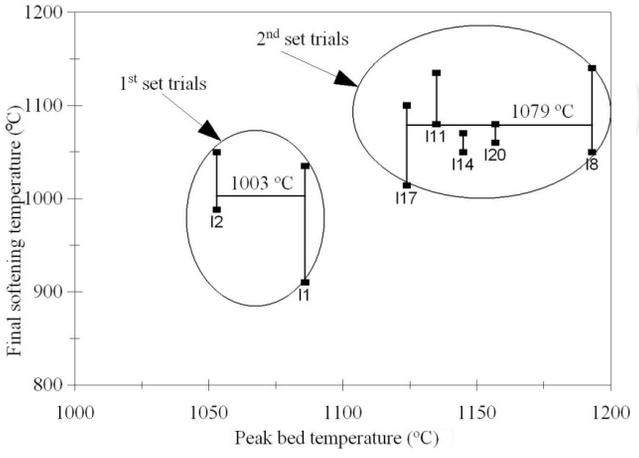

Figure 36. Relationship between final lead sinter softening temperatures and peak bed temperatures at Mount Isa lead sinter plant [19]

http://dx.doi.org/10.5772/54618

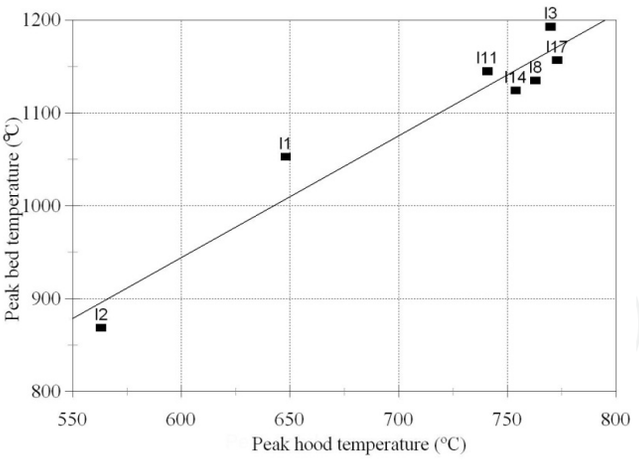

Figure 37. Relationship between peak bed temperatures and peak hood temperatures at Mount Isa lead sinter plant [19]

3. Conclusions

Softening temperature measurements, microstructural, compositional and thermodynamic analysis have been carried out on a range of synthetic and industrial ISF sinters. A simple conceptual has been proposed to assist in understanding the softening behaviour of the complex phase assemblages formed in synthetic and industrial sinters.

The "initial softening temperatures" of ISF sinters are shown to depend principally on the bulk chemical compositions of the materials. There is strong evidence to suggest that in the materials under investigation the initial softening temperatures are related to a critical volume fraction of liquid, equivalent to 30-40 vol% liquid.

The maximum compression and the rate of deformation of the sinters at temperature appear to be directly related to the aspect ratio of the zincite present in the materials; the higher the aspect ratio the lower the deformation rate of the materials. The principal factors determining the formation of plate-like zincite are:

- Peak sinter bed temperature
- Sinter composition

High the aspect ratio zincite is formed by obtaining high iron in solid solution in zincite, this condition is favoured by high iron in the liquid phase, high CaO/SiO_2 ratio and high sintering temperature.

A new wireless temperature probe with four channels has been successfully used on the lead sinter machine at Mount Isa Mines to measure the temperature profile within the sinter bed during operation. Strong correlations have been observed between peak bed temperature and peak hood temperature, and mean sinter softening temperature and peak bed temperature. For the feed material used in the trials, to obtain sinters with mean softening temperatures

above 1050 ºC, peak bed temperatures above 1130 ºC are required. There appears to be a direct correlation between granule size distribution in the feed and peak bed temperature attainable. High peak bed temperatures are observed with narrow feed granule size distribution.

Acknowledgements

Part of the chapter was taken from the following papers, the co-authors of these papers are acknowledged for their contributions.

Zhao B., Burrows A., Jak E. and Hayes P.C., "Microstructures and Softening Behaviours of Lead Sinters and their Correlation to Sintering Temperatures in Mount Isa Lead Smelter", *Transactions of the Institutions of Mining and Metallurgy, Section C: Mineral Processing and Extractive Metallurgy,* Vol. 119(3), 2010, pp. 130-135.

Zhao B., Jak E. and Hayes P.C., "High Temperature Softening Behaviour or ISF Sinters in Air", *Canadian Met. Quart.*, Vol. 47(2), 2008, pp. 139–148.

Author details

Baojun Zhao*

Address all correspondence to: baojun@uq.edu.au

School of Chemical Engineering, The University of Queensland, Brisbane, Australia

References

[1] Noguchi, H. Zinc and Lead Smelting at Hachinohe Smelter. lead-zinc (2010). COM2010, Vancouver, Canada, 2010, , 615-620.

[2] Zhao, B, Jak, E, & Hayes, P. C. High Temperature Softening Behaviour or ISF Sinters in Air. Canadian Met. Quart., (2008). , 47, 139.

[3] Zhao, B, Jak, E, Hayes, P. C, Yang, G, Wang, J, Dong, Y, & Errington, B. Characteristics of ISASMELT Slag and Lead Blast Furnace Sinters. Lead & Zinc'05 Int. Symp., Kyoto, 17-19 Oct (2005). , 571-586.

[4] Holliday, R. J, & Shoobridge, P. H. *The Aus. I.M.M. Conference*, North Queensland, AusIMM, Melbourne, (1978). , 311-321.

[5] Holliday, R. J, Shoobridge, P. H, & Firkin, G. R. *Proc. Australia Japan Extractive Metallurgy Symp.*, Sydney, AusIMM, Melbourne, (1980). , 343-351.

[6] Hayashi, J, Morita, M, Kumagai, H, & Chiba, T. *Fuel*, (2003). , 82, 487-500.

[7] Zhao, B, Jak, E, & Hayes, P. C. *Canadian Met. Quart.*, (2006). , 45, 261-274.

[8] Zhao, B, Jak, E, Hayes, P. C, Holliday, R, & Lee, R. (2005). *Lead & Zinc'05 Int. Symp.*, Kyoto, 17-19 Oct 2005, , 1459-1474.

[9] Jak, E. Degterov SHayes., P.C. and Pelton A.D., *Proceedings of the Fifth International Symposium on Metallurgical Slags and Fluxes*, Iron and Steel Society, AIME, Sydney, publ. Iron and Steel Society, Warrendale, PA, (1997). , 621-628.

[10] Ralls, K. M, Courtners, T. H, & Wulff, J. *Introduction to Materials Science and Engineering*, John Wiley & Sons, (1976). , 400.

[11] Nitta, T, & Kikuta, K. *World Zinc'93*, edited by Matthew I.G., AusIMM, (1993). , 445-451.

[12] Bellot, J. P, Patisson, F, & Ablitzer, D. *Metall. Trans. B.*, (1993). , 24B, 27-38.

[13] Zhao, B, Jak, E, Hayes, P. C, Yang, G, Wang, J, Dong, Y, & Errington, B. Characteristics of Isasmelt Slag and Lead Blast Furnace Sinters', Proc. Pb-Zn'05, Kyoto, Japan, MMIJ, October (2005). , 2005, 571-586.

[14] Cameron, A. W, Eyers, S. A, & Nelson, N. L. The New Updraught Sinter Plant at Mount Isa Mines Limited', Proc. Aust. Inst. Min. Met., No. 226, Part (1968). , 2(1968), 131-149.

[15] Siemon, J. R, Kowalczyk, E, & Tuppurainen, J. The Estimation of Burn-through Point on a Lead Sinter Plant', The 3rd Conference on Control Engineering, Sydney, Australia, Institution of Engineers, Australia, May (1986). , 1986, 191-195.

[16] Siemon, J. R, Tuppurainen, J, & Hollis, R. G. Bed Temperature Prediction in a Lead Sinter Plant', Non-ferrous Smelting Symposium, Port Pirie, Australia, AusIMM, Septmber(1989). , 1989, 27-32.

[17] Jak, E, Zhao, B, Degterov, S, Pelton, A. D, & Hayes, P. C. Coupled Experimental and Thermodynamic Modelling Studies of the System PbO-ZnO-FeO-Fe_2O_3-CaO-SiO_2-Al_2O_3 for Lead and Zinc Smelting', Int'l Conf on Lead/Zinc, Calgary, Canada, CIM, August (1998). , 1998, 313-333.

[18] Jak, E, Degterov, S, Zhao, B, Pelton, A. D, & Hayes, P. C. Coupled Experimental and Thermodynamic Modelling Studies of Slags for Metallurgical Smelting and Coal Combustion Systems', Metall. Mater. Trans. B, (2000). B, , 621-630.

[19] Zhao B., Burrows A., Jak E. and Hayes P.C., "Microstructures and Softening Behaviours of Lead Sinters and their Correlation to Sintering Temperatures in Mount Isa Lead Smelter", *Transactions of the Institutions of Mining and Metallurgy, Section C: Mineral Processing and Extractive Metallurgy,* Vol. 119(3), 2010, pp. 130-135.

IntechOpen